Hindawi Publishing Corporation
Journal of Nanomaterials
Volume 2012, Article ID 452767, 11 pages
doi:10.1155/2012/452767

Research Article

Evaluation on Cartilage Morphology after Intra-Articular Injection of Titanium Dioxide Nanoparticles in Rats

Jiangxue Wang,[1] Yu Gao,[1] Ying Hou,[1] Feng Zhao,[1] Fang Pu,[1] Xiaoyu Liu,[1] Zhihong Wu,[2] and Yubo Fan[1]

[1] *Key Laboratory for Biomechanics and Mechanobiology of the Ministry of Education, School of Biological Science and Medical Engineering, Beihang University, Beijing 100191, China*
[2] *Department of Orthopedics, Peking Union Medical College Hospital, Beijing 100730, China*

Correspondence should be addressed to Yubo Fan, yubofan@buaa.edu.cn

Received 16 November 2011; Accepted 5 January 2012

Academic Editor: Xiaoming Li

Nanoscale wear particles would generate from orthopedic implants with nanoscale surface topography because of residual stress. In this study, the effect of TiO_2 nanoparticles on articular cartilage was investigated by intra-articular injection in rats. Using contrast-enhanced high-resolution microcomputed tomography (micro-CT) technology, the decreased thickness of articular cartilage in distal femur was determined at 1, 7, 14, and 30 days after nanoparticle exposure. A strong linear correlation ($r = 0.928$, $P < 0.0001$) was observed with the results obtained by needle probe testing. After exposure to TiO_2 nanoparticles, cartilage thickness showed time-dependent decrease, and cartilage volume was decreased too. Further, the histopathological examination showed the edema chondrocyte and shrinked nucleus in the radial and calcified zone of cartilage. The ultrastructure of articular cartilage implied that the chondrocyte was degenerated, expressing as the condensed chromatin, the dilated endoplasmic reticulum, and the rich mitochondria. Even, the fragments of ruptured endoplasmic reticulum were observed in the cytoplasm of chondrocytes at postexposure day 30. Results indicate that potential damage of articular cartilage was induced by particles existed in knee joint and imply that the biomonitoring should be strengthened in patients with prostheses replacement.

1. Introduction

The nanoscale (less than 100 nm) surface topography endows nanomaterials as high biological active matrix for protein adsorption and focal attachment [1, 2], which provides a forthcoming prospect in tissue regeneration and orthopedic prostheses [3–5]. Titanium is widely used in hip and joint implants and is biocompatible because it spontaneously forms a protective oxide thin film (TiO_2 coating, typically 4–6 nm thin) at its surface. It is reported that nanoscale coating creates a conditioned interface for osteoblast and chondrocyte adhesion [6–10] and promotes the osteointegration and bone mineralization *in vivo* [11]. However, because of corrosion, fretting, friction, and mechanical loss, many wear particles would generate at the bone-implant interface or in the joint space [12, 13]. Kuster et al. [14] reported that wear particles with lamellar, chunky, osseous, elongated, and rod shapes were observed in healthy and osteoarthritic human knee joints. Except the different shapes, the nanoscale polyethylene wear particles below 0.05 μm and metal wear particles with sizes from 40 to 120 nm containing Co, Cr, and Ti are detected *in vivo* with high-resolution microscopy technology [15, 16]. Many researchers reported that nanoscale particles have a potential impact on living organism [17, 18]. *In vivo*, TiO_2 nanoparticles would be phagocytosed by the epithelial and endothelial cells or macrophages, be translocated into the heart, lung and liver tissues with the blood circulation and cause the oxidative stress and inflammatory response [19, 20]. For the interaction with cells, TiO_2 nanoparticles are generally studied *in vitro* that the DNA damage and cell membrane decomposition are induced by the photocatalysis of TiO_2 [21–23]. In our pilot study, the intra-articular-injected TiO_2 nanoparticles have a potential toxicological effect on the knee joint and could be disseminated to the major organs of rats from joint cavity [24]. The aggregated TiO_2 nanoparticles deposited in the

knee joint induce the synovium hypertrophy, lymphocytes and plasma cells infiltration, fibroblast proliferation, and oxidative damage. However, some studies reported that the inflammatory response occurred in synovium involved in regulating the remodeling of articular cartilage, leading to a loss of cartilage [25, 26].

Articular cartilage is very important in the joint movement for providing a resilient and low-friction bearing surface. The thickness of articular cartilage is related either to the age, to the osteoarthritis, or to the mass of donors. Shepherd and Seedhom [27] reported that thick cartilage existed in the incongruent knee joint where most body weight loaded on. Generally, the cartilage thickness is measured by needle probe, ultrasonic technique, optical stereomicroscope, and magnetic resonance imaging (MRI) technique [28]. MRI technique is successfully used for measuring the articular cartilage thickness of humans [29], but the resolution of current clinical MRI systems (200 μm) is not enough to analyze the small animal models and limits its application. With the needle probe method, the intact, in situ cartilage can be tested.

X-ray microcomputed tomography (μ-CT) is an X-ray-based nondestructive 3D imaging modality with micrometer-level voxel resolutions and quantitative morphological analysis of electron-dense tissues such as tooth and bone of rat, mouse, and rabbit. It is widely used for diagnosing disease in medicine and scientific research in material science, pharmacy, and biology, and so forth. Golding et al. [30] proved that μ-CT is a faster and more accurate spatially 3D technique than histological sections for reconstruction of molluscan anatomy. For soft tissues, the contrast-enhanced technique with iodic-contained solution agent is developed to compensate poor radiopacity and to improve the X-ray images. The successful measurement of kidney volume, length, and thickness in mice was performed *in vivo* and *ex vivo* by Almajdub et al. [31] using the contrast-enhanced high-resolution μ-CT technology as well as the liver and spleen tumor assessment in living mice [32]. Recently, the equilibrium partitioning of an ionic contrast agent via μ-CT (EPIC-μCT) is presented as a noninvasive imaging technique and used to assess the articular cartilage morphology in rabbit [33] and rat model [34].

In this study, the potential influence of intra-articular injected TiO_2 nanoparticles on the articular cartilage in distal femur of rats are investigated at postexposure days 1, 7, 14, and 30. The general approach is to expose rats to the well-characterized nanoparticles by intra-articular injection, to estimate the cartilage thickness and volume with time course using 3D cartilage model which was reconstructed by contrast-enhanced high-resolution μ-CT technology and to assess the potential cartilage injury by morphology analysis.

2. Material and Methods

2.1. Materials. TiO_2 nanomaterials (Hangzhou Wan Jing New Material Co., Ltd.) without any coating were used in this study. Its purity was higher than 99.8%. The properties such as size, crystal profile, and structure state of TiO_2 were well characterized previously [24]. Briefly, TiO_2 nanoparticles were red blood cells-like wafers with the average diameter of 45.87 ± 7.75 nm, the thickness of 10~15 nm, and the average pore size of 7.50 ± 2.58 nm. The crystal profile was pure anatase. The surface area was 105.03 m^2/g with the cumulative pore volume of 0.42 cm^3/g, which was determined under Quadrasorb SI analyzer (Quantachrome Instruments, USA) by N_2 absorption at 77.3 K. In sterile physiological solution, TiO_2 tended to aggregate and clustered from 183.7 to 282.0 nm and from 575.6 to 1018.9 nm.

The contrast agent used in this study was Compound Meglumine Diatrizoate Injection (CMDI, ionic monomer iodic contrast agent, iodine concentration = 370 mg/mL; Shanghai Xudong Haipu Pharmaceutical Co., Ltd, Shanghai) consisting of 32 mg/mL sodium diatrizoate and 268 mg/mL meglumine diatrizoate. The ultrapure water was prepared with a resistivity of 18.2 MΩ*cm (PureLab Plus, Pall, USA). Phenylmethanesulfonyl fluoride (PMSF) was provided by Roche. All other reagents used in this study were at least of analytical grade.

2.2. Animals. Male Sprague Dawley rats with 180–200 g body weight (about 7-8 weeks old, Experimental animal center of Peking University) were housed in polycarbonate cages placed in a ventilated, temperature-controlled room. The standard conditions were supplied and maintained at 20 ± 2°C room temperature, 60 ± 10% relative humidity, and 12 h light/dark cycle. The commercial pellet diet and distilled water for rats were available *ad libitum*. All procedures used in these animal studies were compliant with the local approved protocols of the Administration Office Committee of Laboratory Animal. Animals were acclimated to this environment for five days prior to treatment.

2.3. Experimental Protocol. We prepared TiO_2 suspension using physiological saline solution at 2 mg/mL. Briefly, the powdered TiO_2 nanoparticles were dispersed in the fresh sterilized physiological saline solution, and the suspension was ultrasonicated for 10 min in 4°C at 200 W to disperse completely as much as possible.

The animals' experiments were set at four time intervals (postexposure days 1, 7, 14, and 30) to evaluate the change of articular cartilage thickness and morphology. Based on our previous study [24], both control and nanoparticles-exposed rats were included (10 rats per group) in each time interval because the intra-articular nanoparticles would be disseminated to other tissues. The dosage of 2 mg/kg was selected, which is lower than the detected Ti particles in patients [35]. Before treatment, animals were anesthetized by 30 mg/kg bw i.p. sodium pentobarbital (Germany). The furs on bilateral hind knees were shaved softly after soaking with soaps liquid, and the povidone iodine was applied to prevent infection. The two hind knee joints were intra-articular injected with 100 μL of 2 mg/mL TiO_2 suspensions every other day for 4 times, respectively. TiO_2 suspension was vortexed for 3 min before injections. The equal volume physiological saline solution was given to the control rats. Following the exposure, all rats were held for drink and food *ad libitum*. The daily activity and body weight of all rats were recorded carefully. At postexposure days 1, 7, 14,

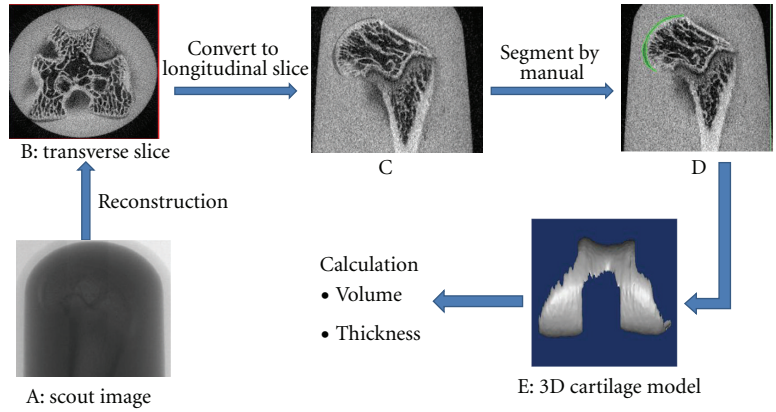

Figure 1: Scanning, segmenting, and remodeling of articular cartilage in distal femur. (A): scout image of distal femur obtained by μ-CT; (B): transverse slice of distal femur; (C): sagittal slice of distal femur; (D): the green part is cartilage; E: 3D cartilage model.

and 30, the hind knee joints were collected both in the control and exposed group. To cut off the peripheral muscle and ligament carefully, six distal femurs from three rats per group were fixed in 10% formalin solution for histopathological analysis. Three fresh cartilages from three rats per group were immediately immersed in 2.5% glutaraldehyde at 4°C for transmission electron microscopy observation. The remainder distal femurs were cut transversely at the midpoint of the femoral neck, wrapped in sterilized gauze which was soaked with phosphate buffered saline (PBS), and then stored in −20°C. To protect the cartilage from degeneration, 0.1 mmol/L PMSF was used in PBS.

2.4. Determination of Contrast Agent Concentration. The concentration of contrast agent is very important for distinguishing the cartilage and calcified bone tissue, segmenting the cartilage contour accurately, and remodeling the cartilage. To determining the optimal contrast agent concentration, the contrast agent CMDI was diluted in different concentration by PBS solution. The four distal femurs from 10-week-old rats additionally was incubated in 5 mL tube containing 20%, 30%, and 40% CMDI dilution of PBS for 10 min at 37°C, then immediately transferred to a μ-CT system for scanning, respectively. All scanning were carried out at 70 kV, 142 μA, and with 18 μm isotropic pixel size.

2.5. Cartilage Scanning and Remodeling. Based on the above determined contrast agent concentration, the incubation in 30% CMDI for 10 min at 37°C was selected as the best protocol. The freezed distal femurs were thawed at 37°C, incubated in 30% CMDI for 10 min, and then scanned with 18 μm isotropic pixel size using SkyScan 1076 microtomograph (Aartselaar, Belgium) at 70 kV, 142 μA. The whole procedure of scanning, segmenting, and remodeling of articular cartilage was shown in Figure 1. The specimen tube was fixed on object bed at horizontal level. After preview, the 35 × 200 mm area was scanned with the source-detector pair rotating with 0.02°/min/step. To enhance tissue features in image, aluminum 1.0 mm physical filter was selected to absorb the low-energy X-ray. The transverse slices of distal femur were reconstructed using cone-beam reconstruction program and transformed to sagittal slices using DataViewer software package (Aartselaar, Belgium). In order to accurately partition the contrast agent, articular cartilage, and calcified bone, the cartilage contour was segmented by manual according to the CT value. Finally, the 3D cartilage model was reconstructed (Figure 1(e)). The 3D cartilage model was imported into the 3D software Geomagic Studio (Raindrop Geomagic Inc., USA) and to calculate the volume of articular cartilage. Because the change of articular cartilage thickness occurred at the femoral weight bearing sites [33], the cartilage thickness was determined at six points on the superior load-bearing aspect of the medial condyle and lateral condyle of femur by virtually sectioning 3D cartilage model at the desired sagittal plane. All scans and analyses were performed by a single-experienced operator.

2.6. Needle Probe Testing. The distal femurs used in μ-CT scanning were potted in dental resin using a cylindrical pot and then used to measure cartilage thickness by needle probe testing. The potted specimen was mounted on a specially designed apparatus that could adjust the articular cartilage surface precisely in five degree-of-freedom directions (x, y, θx, θy, and θz) to perpendicular to the needle probe (Figure 2(a)). The apparatus was positioned on the base groove of an Autograph AG-IS material testing machine (Shimadzu, Japan). Once positioned, the assembly was locked strictly to provide enough rigidity through the tests.

Articular cartilage thickness was measured by slow (0.03 mm/min) insertion of a blunt needle probe (0.5 mm in diameter) attached to a 50 N load sensor (sensitivity: 0.25 N). All tests were conducted at room temperature. In whole test procedure, the cartilage surface was kept hydrated with PBS-containing PMSF. The load and displacement outputs were recorded at 0.05 sec interval as the probe penetrated into the cartilage tissue. A change of the slope of the load-displacement curve indicated the probe penetrated from the cartilage to the calcified bone. Cartilage thickness was measured using the probe to sense the moments when the

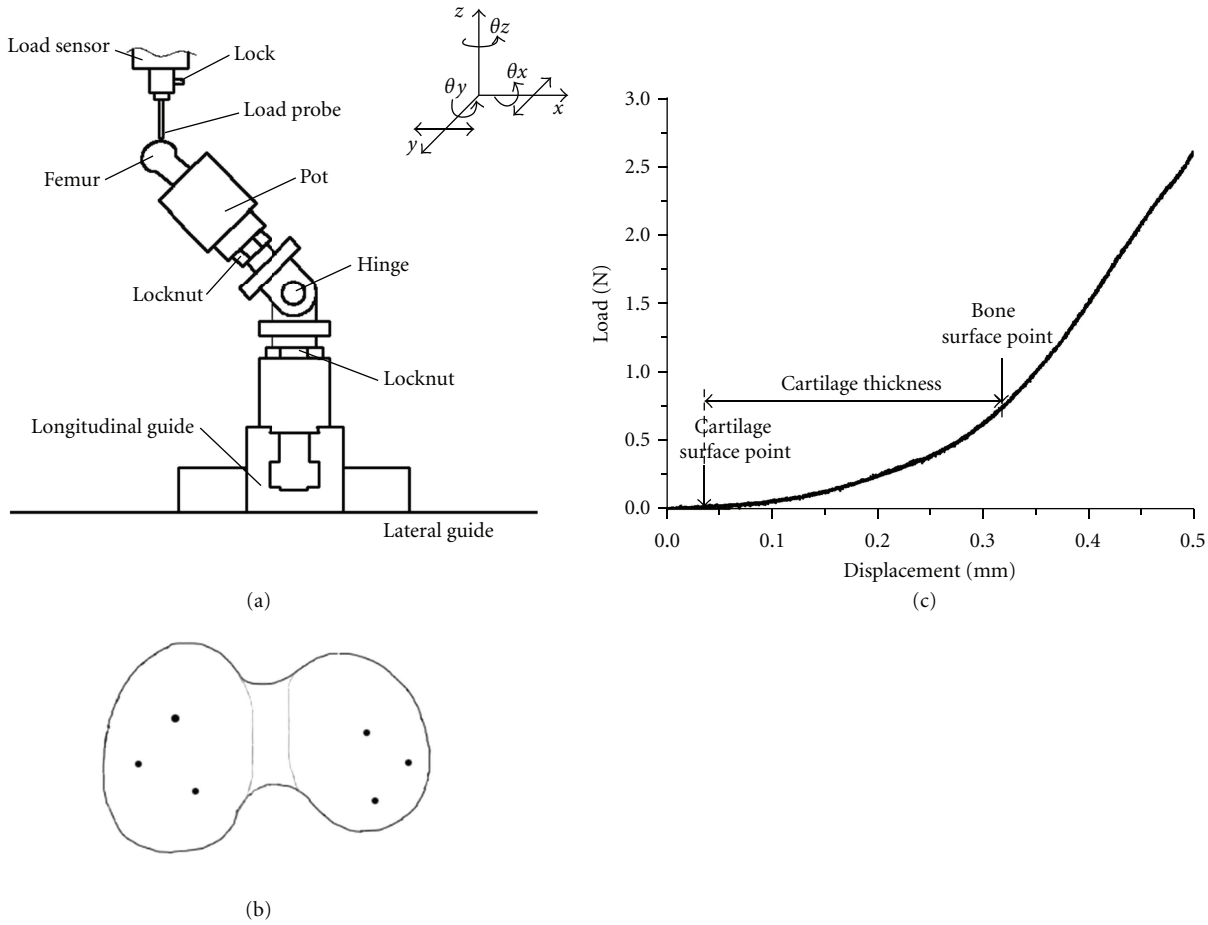

Figure 2: (a) the sketch of specially designed apparatus with five degree-of-freedom direction, (x, y, θx, θy, and θz) adjustment of articular cartilage surface perpendicular to the load probe (b) the six points on the superior load bearing aspect of the medial condyle and lateral condyle of distal femur, which is subjected to needle probe tests (c) the representative load-displacement curve.

probe pressed the articular surface and when it contacted the calcified bone (Figure 2(c)). Needle probe testing was performed at six points on the medial condyle and lateral condyle of femur (Figure 2(b)) in corresponding to the sites on 3D cartilage model.

2.7. Histopathology Examination of Articular Cartilage. The distal femurs were fixed in 10% formalin solution, decalcified with 10% nitric acid for 24 h, and rinsed by tap water for 4 h. And then, the histopathological tests were performed using standard laboratory procedures. Briefly, the tissues were dehydrated in graded series of 80%, 90%, 95%, and 100% ethanol, followed by clearing in toluene, infiltrated in hot liquid paraffin, finally embedded in paraffin blocks to allow for 5 μm sections, and mounted onto the glass slides. They were stained with hematoxylin-eosin (H&E) for microscopic analysis. All sections were observed, and the photos were taken using optical microscope (Olympus BX51, USA). The identity and analysis of pathology sections were blind to the pathologist.

2.8. Ultrastructure of Cartilage by Transmission Electron Microscopy. The fresh cartilage was carefully cut off by scalpel and immediately immersed in 2.5% glutaraldehyde at 4°C. After washing with PBS sufficiently, the cartilage was fixed with 1% osmium tetroxide, dehydrated in a graded series of ethanol, embedded in araldite, and polymerized for 24 h at 37°C. Ultrathin sections (50 nm) were cut with ultramicrotome (LKB-V, Sweden), contrasted with uranyl acetate and lead citrate, and observed with TEM (H-600, Hitachi).

2.9. Statistical Analysis. For statistical analysis, all data are expressed as mean ± standard deviation (SD). The one-way analysis of variance (ANOVA) was performed to analyze the significance using the statistical software SPSS 13.0 for windows. A LSD post hoc multiple comparison test was used for different groups. $P < 0.05$ was considered as the statistical significance.

3. Results

3.1. Concentration of Contrast Agent. According to the different X-ray attenuation (CT value) of contrast agent, cartilage and calcified bone, the optimal contrast agent concentration was determined. Figure 3 showed the representative saggittal

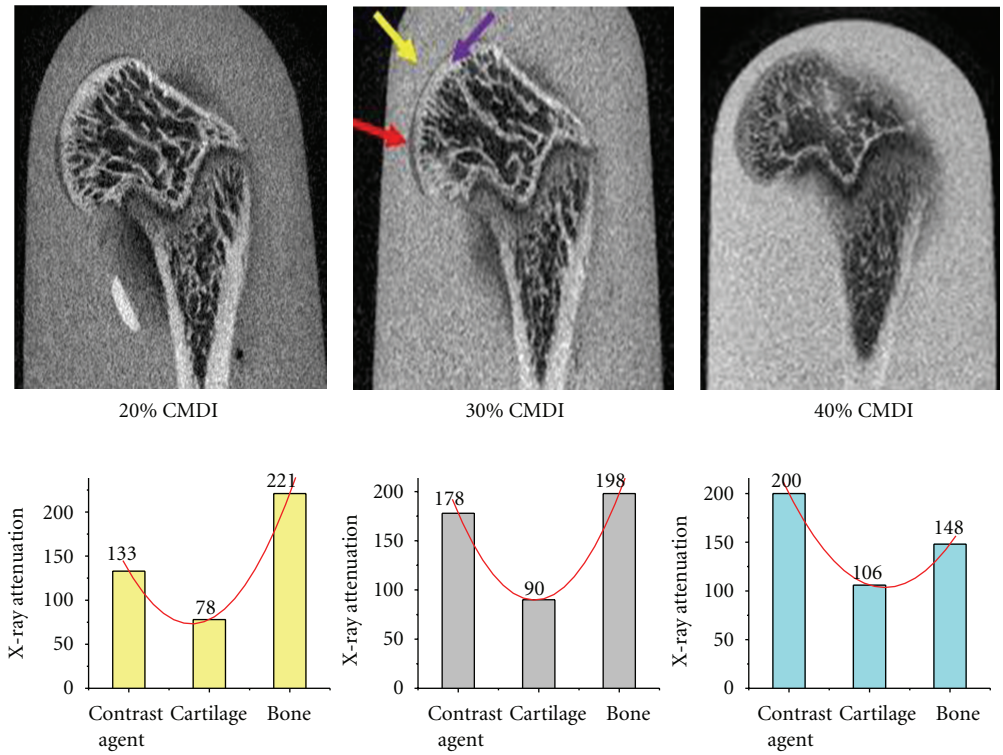

FIGURE 3: The representative sagittal slice of distal femur in 20%, 30%, and 40% CMDI for μ-CT in the rat model, the average X-ray attenuation of contrast agent, articular cartilage, and calcified bone in the corresponding CMDI. Yellow, red, and purple arrows refer to the contrast agent, articular cartilage, and calcified bone, respectively.

slice of distal femur in 20%, 30%, and 40% CMDI for μ-CT in the rat model and the average X-ray attenuation of contrast agent, articular cartilage, and calcified bone in the corresponding CMDI. In 20% CMDI, the average X-ray attenuation of femoral articular cartilage and calcified bone was 78 and 221, respectively. This contrast difference was enough to segment the cartilage from calcified bone, but not enough to differentiate the cartilage from contrast agent accurately. In 40% CMDI, the average X-ray attenuation of cartilage was 106, which was close to that of calcified bone (148). Therefore, it was difficult to distinguish between the cartilage and calcified bone in segmenting by manual. However, when the distal femur was incubated in 30% CMDI, the average X-ray attenuation of contrast agent, cartilage, and calcified bone was 178, 90, and 198, respectively, which provided the appropriate contrast difference for accurately segmenting the cartilage from the contrast agent and calcified bone. In the following scanning, therefore, all the distal femurs were incubated in 30% CMDI to remodel the cartilage.

3.2. Thickness and Volume of Articular Cartilage Determined by μ-CT. According to the above-determined concentration of contrast agent, the incubation in 30% CMDI for 10 min at 37°C was selected as the best protocol. Three distal femurs per group were scanned to obtain the 3D cartilage model. The thickness of articular cartilage exposed to TiO_2 nanoparticles were calculated and shown in Figure 4. At day 1 after exposure to TiO_2 nanoparticles, the thickness of articular cartilage was 0.2754 ± 0.0207 mm, which was smaller than that of the corresponding control (0.2942 ± 0.0150 mm). The changes in cartilage thickness were calculated comparing with that in the corresponding control at each particular time point. The % reduction was calculated as follows.

$$\%\ \text{reduction} = \frac{(\text{thickness in the corresponding control} - \text{thickness in } TiO_2 \text{ exposed rats})}{\text{thickness in the corresponding control}} * 100 \quad (1)$$

At postexposure days 1, 7, 14, and 30, the thickness of articular cartilage was reduced with the rate of 6.41%, 4.52%, 8.64%, and 11.03%, respectively. Comparing with the corresponding control, the significant difference was detected in rats at days 7, 14, and 30 after exposure to TiO_2 nanoparticles ($P < 0.05$) (Figure 4).

Using the 3D cartilage model, the volume of articular cartilage covered on the distal femur was measured and

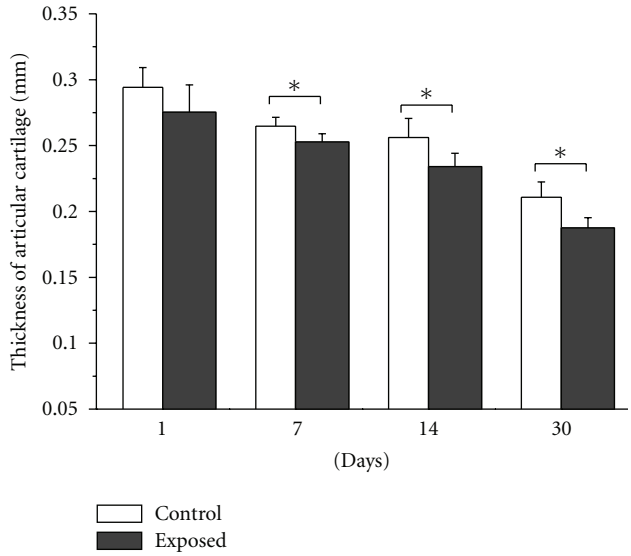

Figure 4: Thickness of articular cartilage in the distal femur by 3D cartilage model. $^*P < 0.05$ compared with the corresponding control.

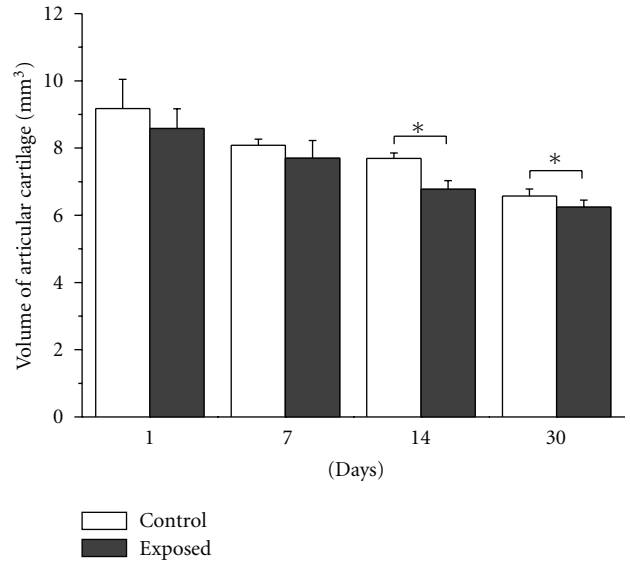

Figure 5: Volume of articular cartilage in the distal femur by 3D cartilage model. $^*P < 0.05$ compared with the corresponding control.

illustrated in Figure 5. At postexposure days 1 and 7, the volume of cartilage showed a little decrease compared to the corresponding control ($P > 0.05$); whereas, at days 14 and 30, the significant reduced cartilage volume was detected ($P < 0.05$). It indicated that the growth of articular cartilage might be disturbed by TiO_2 nanoparticles existed in the joint cavity.

For the control rats at different time points, we determined that the thickness and volume of articular cartilage decreased with the rat age. This was important in cartilage development and consistent with the reported results

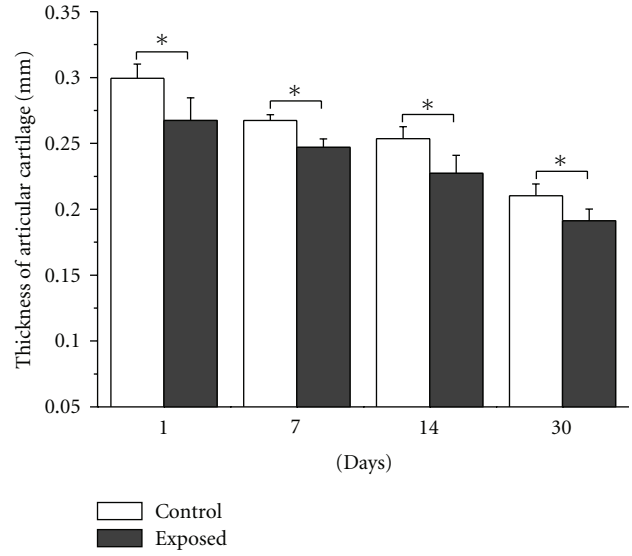

Figure 6: Thickness of articular cartilage in the distal femur by needle probe testing. $^*P < 0.05$ compared with the corresponding control.

[34, 35], which could be due to the endochondral bone development and fibrillation under function adaptation or physiological adaptation in rats during normal growth.

3.3. Thickness of Articular Cartilage Detected by Needle Probe Testing. In testing, the load-displacement curves were recorded as the load probe penetrated to the cartilage with 0.03 mm/min. According to the slope change of the load-displacement curve, the thickness of articular cartilage in distal femur of rats in each group was determined and illustrated in Figure 6. For the control rats, the thickness of articular cartilage became reduced with the rat age increase, which was consistent with the results obtained by the 3D cartilage model. For the rats exposed to TiO_2 nanoparticles, the cartilage thickness showed the significant decrease compared to the corresponding control ($P < 0.05$) at postexposure days 1, 7, 14, and 30, respectively.

These results showed a strong linear correlation ($r = 0.928$, $P < 0.0001$, $n = 48$) with that determined by the 3D cartilage model (Figure 7), which suggested that the determination of cartilage thickness obtained both by 3D cartilage model and by needle probe testing was accurate and creditable.

3.4. Morphology Change of Articular Cartilage. In whole exposure and postexposure period, animals were given food and water *ad libitum*, no abnormal daily activity was observed. After sacrificing the rats, the smooth and moist knee cavity including synovial capsule were observed in the control rats; whereas, the white particles-xanthoproteic complexes were observed in the synovial joint capsule of exposed rats, which indicated the deposition of intra-articular TiO_2 particles. With the time prolong from the postexposure days 1 to 30, the deposited particles-xanthoproteic complexes were reduced, as shown in Figure 8.

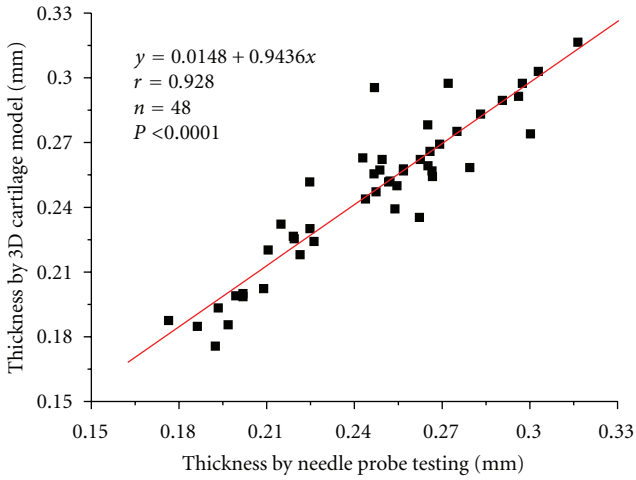

Figure 7: The linear correlation between the values of cartilage thickness obtained by 3D cartilage model and needle probe testing. The correlation function $y = 0.0148 + 0.9436$, and $P < 0.0001$ showed a strong linear correlation ($r = 0.928$).

The histopathology of articular cartilage by H&E staining was shown in Figure 9. Both in the control and exposed rats, the articular cartilage had the intact perichondrium and homogenous cartilage matrix. Depending on the arrangement of chondrocytes and collagen fibres, articular cartilage is divided into several zones including the tangential layer, the transitional zone, the radial zone, and the calcified cartilage layer. In the control, the matrix of the calcified cartilage layer stained slightly darker than the matrix of the other cartilage zones. However, at postexposure day 30, the calcified cartilage layer was eosin-stained, which stained lighter than that of the other groups. In the radial and calcified zone of the cartilage, the chondrocyte was edema, and the cell nucleus was shrinked. These implied that the cartilage injury was induced by the intervention of deposited TiO_2 nanoparticles at day 30.

Figure 10 showed the ultrastructure of articular cartilage in the distal femur observed by TEM. After exposure to TiO_2 nanoparticles, the chromatin was condensed and distributed over the fringe of nucleus, the nuclear membrane was invaginated, endoplasmic reticulum was dilated, and ribosomes were decreased in chondrocyte at day 1. The rough endoplasmic reticulum had a lamellar arrangement in the cytoplasm at days 7. The intense axons on the cell surface were developed, and the mitochondria were rich and became swollen in chrondrocyte at day 14. At postexposure day 30, to our surprise, the endoplasmic reticulum ruptured, and the fragments were distributed in the cytoplasm.

4. Discussion

Herein, the impact of TiO_2 nanoparticles on the articular cartilage in the knee joint was reported. By intra-articular injecting the nanoscale TiO_2 suspension, we observed that there was some particles deposition in the knee joint of rats. Using contrast-enhanced high-resolution μ-CT technology, we determined that the cartilage thickness decreased significantly at postexposure days 7, 14, and 30, which has a strong linear correlation ($r = 0.928$, $P < 0.0001$) with the results obtained by needle probe testing. It is reported that the cartilage change would occur on the medial condyle and lateral condyle of femur because of the compression from weight [36]. Articular cartilage is the smooth, glistening white tissue that covers the surface of all the diarthrodial joints. The main structure of cartilage is the "Benninghoff" collagenous fibre (mainly type II collagen) and the hydrated proteoglycan embedded in it to provide the proper biomechanical function. In our previous study [24], the intra-articular TiO_2 nanoparticles resulted in the synovium hypotrophy, oxidative damage, and inflammation, such as lymphocytes and plasma cells infiltration and fibroblast proliferation. Some studies reported that the inflammatory response occurred in synovium was involved in regulating the remodeling of articular cartilage and affecting the chondrocyte function, leading to a loss of cartilage and erosion and weakness of the bones [25, 26]. It is to say that the activated synovial fibroblasts attached to the pannus-cartilage interface and released matrix-degrading enzymes, such as matrix metalloproteinases and the proinflammatory cytokines (TNF-α and IL-1) [26, 37]. The matrix-degrading enzymes would inhibit the synthesis of type II collagen through regulating the chondrocyte and the aggregation of proteoglycans [38]. The reduced extracellular matrix would lead to the thinner articular cartilage. Therefore, in this study, the significant decreased articular cartilage thickness was detected in the distal femur of rats exposed to intra-articular TiO_2 nanoparticles. As determined by the 3D cartilage model, the cartilage thickness reduced about 4.52%, 8.64%, and 11.03% at postexposure days 7, 14, and 30, respectively.

It needs to be pointed out that the thickness and volume of articular cartilage in the control rats also showed a reduction with age. In the weight-bearing joint, studies reported that the cartilage thickness reduced with age both in human [36, 39] and in horse [40]. This is important in cartilage development and ascribed to the endochondral bone development and fibrillation under functional or physiological adaptation. The fetal cartilage is homogenous, showing no site-dependent differences. As the animal gets older and cartilage maturates, cartilage becomes gradually heterogeneous under the influence of joint loading, showing topographical variations in both thickness and compressive stiffness. It is worth to emphasize that Xie et al. [34] also showed that the thickness and volume of cartilage in distal femur decreased in rat during normal growth from 4 to 8 weeks, and even to 16 weeks.

As the only living element of the articular cartilage, the chondrocyte holds a key position in the development of cartilage. It produces the components of the matrix, that is, collagens and proteoglycans. Therefore, besides the above determination of the articular cartilage thickness, the histopathology and ultrastructure of articular cartilage were analyzed in this study to observe the change of chondrocytes after exposure to TiO_2 nanoparticles. Results showed that the chondrocytes were edema and degenerated

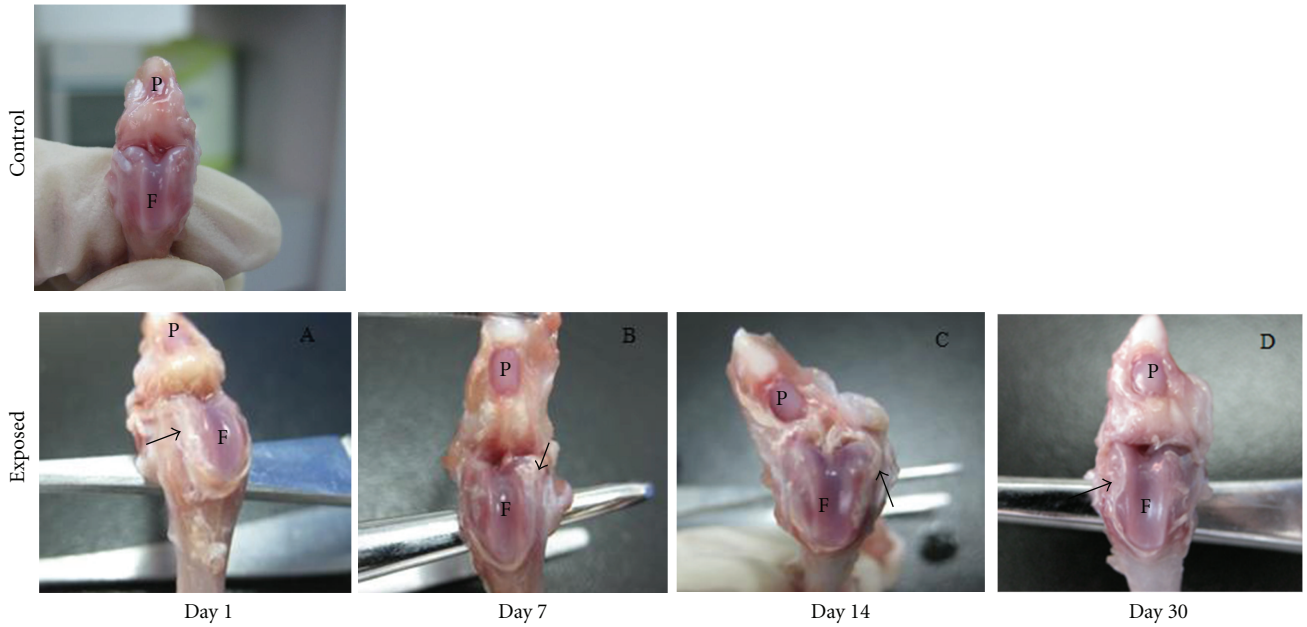

Figure 8: Photograph of knee joint cavity in rats after intra-articular injection of TiO_2 nanoparticles. Control: the smooth and moist knee cavity; exposed: the white particles-xanthoproteic complexes (arrows) in the synovial joint capsule of exposed rats, which indicate the deposition of TiO_2 particles. With the time prolong from the postexposure days 1 to 30, the deposited particles-xanthoproteic complexes were reduced. P: patellar; F: femur.

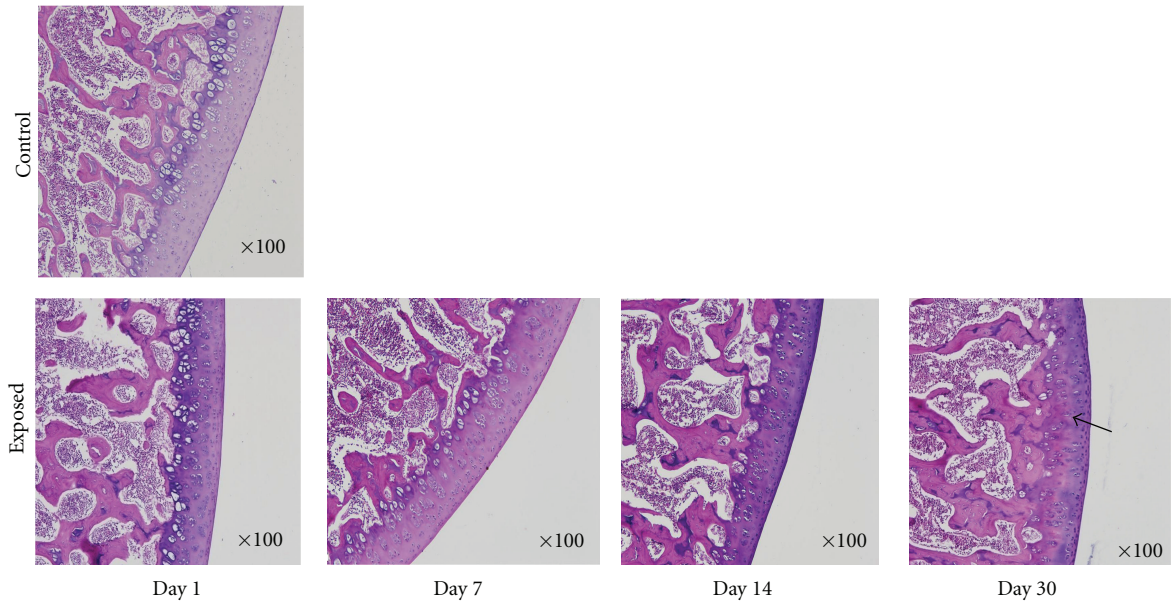

Figure 9: Microphotograph of articular cartilage in the distal femur exposed to TiO_2 nanoparticles by H&E staining. Arrow indicates the edema and degenerated chondrocytes in the radial and calcified zone at postexposure day 30.

in the radial and calcified zone at postexposure day 30. The ultrastructural study of cartilage suggested the degeneration of chondrocyte. More importantly, the mitochondria were rich and became swollen in chondrocyte at postexposure day 14; the endoplasmic reticulum were ruptured in the chondrocyte at postexposure day 30. It is well known that the endoplasmic reticulum plays an important role in the hydroxylation and glycosylation of procollagen, and the mitochondrion takes part in oxidative phosphorylation and functions as the energy factory of cell. The ruptured endoplasmic reticulum would inhibit the synthesis of collagen and glycosaminoglycans [41]. The reduction in matrix synthesis may provide a potential explanation for the thinning of articular cartilage observed in our study. Further, it is reported that chondrocyte promotes the articular cartilage loss because the surface receptors for cytokines respond to

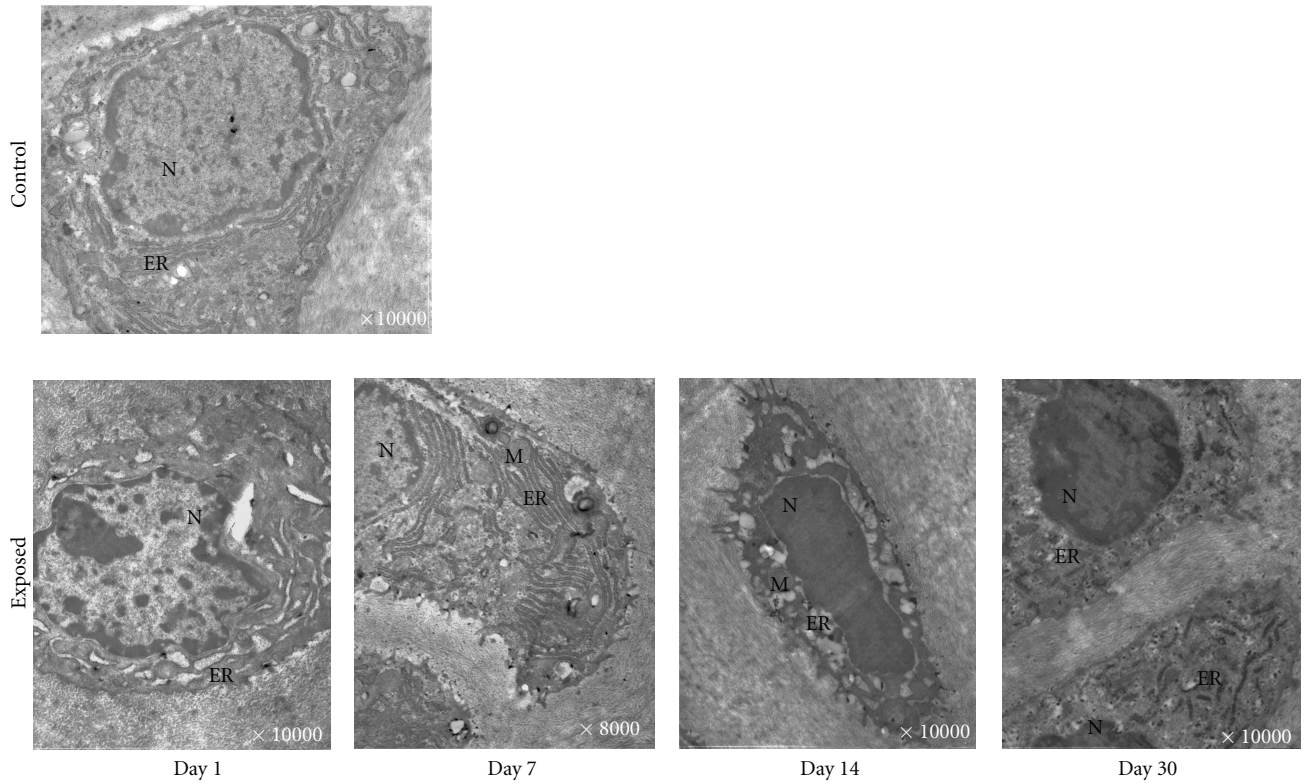

Figure 10: The ultrastructure of articular cartilage in the distal femur exposed to TiO_2 nanoparticles. N: nucleaus; ER: endoplasmic reticulum; M: mitochondria. After TiO_2 nanoparticles exposure, the chromatin was condensed and distributed over the fringe of nucleus, the nuclear membrane was invaginated, the endoplasmic reticulum was dilated, and the ribosomes were decreased in chondrocyte at postexposure day 1. At day 7, a lamellar arrangement for rough endoplasmic reticulum was observed in cytoplasm. At day 14, the intense axons on the cell surface were developed and the mitochondria were rich and became swollen in chondrocyte. At day 30, the endoplasmic reticulum ruptured, and the fragments were distributed in cytoplasm.

the ligands with the production of prostaglandin E_2 and metalloproteinases in synovitis [42]. Of course, to unveil the detailed mechanism of cartilage loss, it is necessary to further research the influence of nanoparticles on the synthesis of extracellular matrix in cartilage, including the collagen and proteoglycan.

5. Conclusion

In conclusion, after intra-articular injection of TiO_2 nanoparticles, we determined that the thickness of articular cartilage was decreased using contrast-enhanced high-resolution μ-CT technology, which had a strong linear correlation ($r = 0.928$, $P < 0.0001$) with the results obtained by needle probe testing. The cartilage thickness was significant decreased with the rat age, and the same trend was observed in cartilage volume. The analysis of morphology and ultrastructure of articular cartilage indicated the chondrocyte was degenerated. Results suggested that the articular cartilage is a potential target for wear particles in knee joint.

Acknowledgments

This paper is financially supported by the National Natural Science Foundation of China (Grant nos. 30800217, 10925208, and 11032012) and the Postdoctoral Science Foundation of China (20080430304).

References

[1] J. Park, S. Bauer, K. von der Mark, and P. Schmuki, "Nanosize and vitality: TiO_2 nanotube diameter directs cell fate," *Nano Letters*, vol. 7, no. 6, pp. 1686–1691, 2007.

[2] X. Li, C. A. van Blitterswijk, Q. Feng, F. Cui, and F. Watari, "The effect of calcium phosphate microstructure on bone-related cells in vitro," *Biomaterials*, vol. 29, no. 23, pp. 3306–3316, 2008.

[3] R. N. Shah, N. A. Shah, M. M. D. R. Lim, C. Hsieh, G. Nuber, and S. I. Stupp, "Supramolecular design of self-assembling nanofibers for cartilage regeneration," *Proceedings of the National Academy of Sciences of the United States of America*, vol. 107, no. 8, pp. 3293–3298, 2010.

[4] E. Engel, A. Michiardi, M. Navarro, D. Lacroix, and J. A. Planell, "Nanotechnology in regenerative medicine: the materials side," *Trends in Biotechnology*, vol. 26, no. 1, pp. 39–47, 2008.

[5] X. Li, Q. Feng, X. Liu, W. Dong, and F. Cui, "Collagen-based implants reinforced by chitin fibres in a goat shank bone defect model," *Biomaterials*, vol. 27, no. 9, pp. 1917–1923, 2006.

[6] B. D. Boyan, T. W. Hummert, D. D. Dean, and Z. Schwartz, "Role of material surfaces in regulating bone and cartilage cell response," *Biomaterials*, vol. 17, no. 2, pp. 137–146, 1996.

[7] K. Burns, C. Yao, and T. J. Webster, "Increased chondrocyte adhesion on nanotubular anodized titanium," *Journal of Biomedical Materials Research—Part A*, vol. 88, no. 3, pp. 561–568, 2009.

[8] X. Li, Y. Fan, and F. Watari, "Current investigations into carbon nanotubes for biomedical application," *Biomedical Materials*, vol. 5, no. 2, Article ID 022001, 2010.

[9] X. Li, H. Gao, M. Uo et al., "Effect of carbon nanotubes on cellular functions in vitro," *Journal of Biomedical Materials Research—Part A*, vol. 91, no. 1, pp. 132–139, 2009.

[10] X. Li, H. Gao, M. Uo et al., "Maturation of osteoblast-like SaoS2 induced by carbon nanotubes," *Biomedical Materials*, vol. 4, no. 1, Article ID 015005, 2009.

[11] G. Giavaresi, L. Ambrosio, G. A. Battiston et al., "Histomorphometric, ultrastructural and microhardness evaluation of the osseointegration of a nanostructured titanium oxide coating by metal-organic chemical vapour deposition: an in vivo study," *Biomaterials*, vol. 25, no. 25, pp. 5583–5591, 2004.

[12] A. Hatton, J. E. Nevelos, J. B. Matthews, J. Fisher, and E. Ingham, "Effects of clinically relevant alumina ceramic wear particles on TNF-α production by human peripheral blood mononuclear phagocytes," *Biomaterials*, vol. 24, no. 7, pp. 1193–1204, 2003.

[13] R. Niimi, M. Hasegawa, A. Sudo, and A. Uchida, "A large metallic cyst caused by wear particles after total knee arthroplasty," *Archives of Orthopaedic and Trauma Surgery*, vol. 127, no. 1, pp. 51–54, 2007.

[14] M. S. Kuster, P. Podsiadlo, and G. W. Stachowiak, "Shape of wear particles found in human knee joints and their relationship to osteoarthritis," *British Journal of Rheumatology*, vol. 37, no. 9, pp. 978–984, 1998.

[15] M. Lapcikova, M. Slouf, J. Dybal et al., "Nanometer size wear debris generated from ultra high molecular weight polyethylene in vivo," *Wear*, vol. 266, no. 1-2, pp. 349–355, 2009.

[16] I. Milošev and M. Remškar, "In vivo production of nanosized metal wear debris formed by tribochemical reaction as confirmed by high-resolution TEM and XPS analyses," *Journal of Biomedical Materials Research—Part A*, vol. 91, no. 4, pp. 1100–1110, 2009.

[17] A. Nel, T. Xia, L. Mädler, and N. Li, "Toxic potential of materials at the nanolevel," *Science*, vol. 311, no. 5761, pp. 622–627, 2006.

[18] D. B. Warheit, R. A. Hoke, C. Finlay, E. M. Donner, K. L. Reed, and C. M. Sayes, "Development of a base set of toxicity tests using ultrafine TiO_2 particles as a component of nanoparticle risk management," *Toxicology Letters*, vol. 171, no. 3, pp. 99–110, 2007.

[19] V. Stone and K. Donaldson, "Nanotoxicology: signs of stress," *Nature Nanotechnology*, vol. 1, no. 1, pp. 23–24, 2006.

[20] J. Wang, Y. Liu, F. Jiao et al., "Time-dependent translocation and potential impairment on central nervous system by intranasally instilled TiO_2 nanoparticles," *Toxicology*, vol. 254, no. 1-2, pp. 82–90, 2008.

[21] Z. X. Lu, L. Zhou, Z. L. Zhang et al., "Cell damage induced by photocatalysis of TiO_2 thin films," *Langmuir*, vol. 19, no. 21, pp. 8765–8768, 2003.

[22] W. G. Wamer, J. J. Yin, and R. R. Wei, "Oxidative damage to nucleic acids photosensitized by titanium dioxide," *Free Radical Biology and Medicine*, vol. 23, no. 6, pp. 851–858, 1997.

[23] S. Hussain, S. Boland, A. Baeza-Squiban et al., "Oxidative stress and proinflammatory effects of carbon black and titanium dioxide nanoparticles: role of particle surface area and internalized amount," *Toxicology*, vol. 260, no. 1–3, pp. 142–149, 2009.

[24] J. X. Wang, Y. B. Fan, Y. Gao, Q. H. Hu, and T. C. Wang, "TiO_2 nanoparticles translocation and potential toxicological effect in rats after intraarticular injection," *Biomaterials*, vol. 30, no. 27, pp. 4590–4600, 2009.

[25] S. R. Goldring, "Pathogenesis of bone and cartilage destruction in rheumatoid arthritis," *Rheumatology*, vol. 42, no. 2, pp. ii11–ii16, 2003.

[26] F. Rannou, M. François, M. T. Corvol, and F. Berenbaum, "Cartilage breakdown in rheumatoid arthritis," *Joint Bone Spine*, vol. 73, no. 1, pp. 29–36, 2006.

[27] D. E. T. Shepherd and B. B. Seedhom, "Thickness of human articular cartilage in joints of the lower limb," *Annals of the Rheumatic Diseases*, vol. 58, no. 1, pp. 27–34, 1999.

[28] J. S. Jurvelin, T. Räsänen, P. Kolmonens, and T. Lyyra, "Comparison of optical, needle probe and ultrasonic techniques for the measurement of articular cartilage thickness," *Journal of Biomechanics*, vol. 28, no. 2, pp. 231–235, 1995.

[29] F. Eckstein, H. Sittek, S. Milz et al., "The potential of magnetic resonance imaging (MRI) for quantifying articular cartilage thickness—a methodological study," *Clinical Biomechanics*, vol. 10, no. 8, pp. 434–440, 1995.

[30] R. E. Golding, W. F. Ponder, and M. Byrne, "Three-dimensional reconstruction of the odontophoral cartilages of caenogastropoda (mollusca: gastropoda) using micro-ct: morphology and phylogenetic significance," *Journal of Morphology*, vol. 270, no. 5, pp. 558–587, 2009.

[31] M. Almajdub, L. Magnier, L. Juillard, and M. Janier, "Kidney volume quantification using contrast-enhanced in vivo X-ray micro-CT in mice," *Contrast Media and Molecular Imaging*, vol. 3, no. 3, pp. 120–126, 2008.

[32] M. Almajdub, M. Nejjari, G. Poncet et al., "In-vivo high-resolution X-ray microtomography for liver and spleen tumor assessment in mice," *Contrast Media and Molecular Imaging*, vol. 2, no. 2, pp. 88–93, 2007.

[33] A. W. Palmer, R. E. Guldberg, and M. E. Levenston, "Analysis of cartilage matrix fixed charge density and three-dimensional morphology via contrast-enhanced microcomputed tomography," *Proceedings of the National Academy of Sciences of the United States of America*, vol. 103, no. 51, pp. 19255–19260, 2006.

[34] L. Xie, A. S. P. Lin, M. E. Levenston, and R. E. Guldberg, "Quantitative assessment of articular cartilage morphology via EPIC-μCT," *Osteoarthritis and Cartilage*, vol. 17, no. 3, pp. 313–320, 2009.

[35] H. J. Agins, N. W. Alcock, M. Bansal et al., "Metallic wear in failed titanium-alloy total hip replacements. A histological and quantitative analysis," *Journal of Bone and Joint Surgery—Series A*, vol. 70, no. 3, pp. 347–356, 1988.

[36] R. L. Karvonen, W. G. Negendank, R. A. Teitge, A. H. Reed, P. R. Miller, and F. Fernandez- Madrid, "Factors affecting articular cartilage thickness in osteoarthritis and aging," *Journal of Rheumatology*, vol. 21, no. 7, pp. 1310–1318, 1994.

[37] W. H. van der Laan, P. H. A. Quax, C. A. Seemayer et al., "Cartilage degradation and invasion by rheumatoid synovial fibroblasts is inhibited by gene transfer of TIMP-1 and TIMP-3," *Gene Therapy*, vol. 10, no. 3, pp. 234–242, 2003.

[38] P. Seckinger, I. Yaron, F. A. Meyer, M. Yaron, and J. M. Dayer, "Modulation of the effects of interleukin-1 on glycosaminoglycan synthesis by the urine-derived interleukin-1 inhibitor,

but not by interleukin-6," *Arthritis and Rheumatism*, vol. 33, no. 12, pp. 1807–1814, 1990.

[39] G. Meachim, G. Bentley, and R. Baker, "Effect of age on thickness of adult patellar articular cartilage," *Annals of the Rheumatic Diseases*, vol. 36, no. 6, pp. 563–568, 1977.

[40] H. Brommer, P. A. J. Brama, M. S. Laasanen, H. J. Helminen, P. R. Van Weeren, and J. S. Jurvelin, "Functional adaptation of articular cartilage from birth to maturity under the influence of loading: a biomechanical analysis," *Equine Veterinary Journal*, vol. 37, no. 2, pp. 148–154, 2005.

[41] N. Mitchell and N. Shepard, "The ultrastructure of articular cartilage in rheumatoid arthritis. A preliminary report," *Journal of Bone and Joint Surgery—Series A*, vol. 52, no. 7, pp. 1405–1423, 1970.

[42] H. A. Kim and Y. W. Song, "Apoptotic chondrocyte death in rheumatoid arthritis," *Arthritis and Rheumatism*, vol. 42, no. 7, pp. 1528–1537, 1999.